https://doi.org/10.5194/egusphere-2023-1797
Preprint. Discussion started: 5 September 2023
© Author(s) 2023. CC BY 4.0 License.

Technical Note: two-component *E*lectrical *C*onductivity-based hydrograph separa*T*ion employing an *EXP*onential mixing model (*EXPECT*) provides reliable high temporal resolution young water fraction estimates in three small Swiss catchments

Alessio Gentile[1], Jana von Freyberg[2,3], Davide Gisolo[1], Davide Canone[1], and Stefano Ferraris[1]

[1]Interuniversity Department of Regional and Urban Studies and Planning (DIST), Politecnico and Università degli Studi di Torino, 10125, Torino, Italy
[2]School of Architecture, Civil and Environmental Engineering, EPFL, 1015, Lausanne, Switzerland
[3]Mountain Hydrology and Mass Movements, Swiss Federal Institute for Forest, Snow and Landscape Research (WSL), 8903, Birmensdorf, Switzerland

Correspondence to: Alessio Gentile (alessio.gentile@polito.it)

Abstract. The young water fraction represents the fraction of water molecules in a stream that have entered the catchment relatively recently, typically within 2-3 months. It can be reliably estimated in spatially heterogeneous and nonstationary catchments from the amplitude ratio of seasonal isotope ($\delta^{18}O$ or $\delta^{2}H$) cycles of streamwater and precipitation, respectively. It has been found that young water fractions increase with discharge, thus reflecting increased direct runoff with wetter catchment conditions. This so-called discharge sensitivity of the young water fraction (S^*_d) can be useful for describing and comparing catchments' hydrological behaviour; however, the estimation of S^*_d can be highly uncertain and unreliable when the streamwater isotope data are sparse and don't capture the entire flow regime.

Here, we present a new method that can increase the temporal resolution of the young water fraction estimates, and thus better constrain the estimation of S^*_d. Our so-called *EXPECT* method is built upon three key assumptions: 1) the two-component hydrograph separation technique can be used to obtain the portion of young water and old water in a stream by considering EC as a proxy of the water age, 2) the EC value of the young water endmember (EC_{yw}) is lower than that of the old water endmember (EC_{ow}), and 3) the mixing of young water and old water fractions is described assuming an exponential decay of electrical conductivity with increasing young water fraction. We calibrate the two endmembers, EC_{yw} and EC_{ow}, by constraining the time-weighted and flow-weighted average young water fraction achieved with hydrograph separation to be equal to the same quantities obtained from seasonal isotope cycles.

We test the *EXPECT* method with data from three small experimental catchments in the Swiss Alptal valley by using two different temporal resolutions of Q and EC data: sampling-resolution (i.e., we only consider Q and EC measurements during dates of isotope sampling) and daily-resolution. By leveraging high-resolution and low-cost EC measurements and bi-weekly isotope data, the *EXPECT* method has provided reliable young water fraction estimates at bi-weekly and daily resolution, from which S^*_d could be determined with higher accuracy compared to the existing method that uses only bi-weekly isotope

https://doi.org/10.5194/egusphere-2023-1797
Preprint. Discussion started: 5 September 2023
© Author(s) 2023. CC BY 4.0 License.

data. For proper use of the *EXPECT* method, we further highlight its main limitations that may vary in their relevance depending on the characteristics of the catchments under study.

1 1 Introduction

Environmental tracers in catchment studies are used for understanding the age, the origin, and pathways of water in natural environments (Kendall and McDonnell, 1998). Among tracers, hydrologists use the stable water isotopes (^{18}O and ^{2}H) because they are constituent part of the water molecules and hence they are naturally present in precipitation (Kendall and McDonnell, 1998). The isotopic composition in precipitation generally shows a pronounced seasonal cycle (Dansgaard, 1964). Catchment storage acts as a filter on this input seasonal cycle, so that the isotope cycle in streamwater is damped and lagged compared to that in precipitation (McGuire and McDonnell, 2006). The delay and damping we observe in the streamwater cycle is caused by the advection and dispersion of stable water isotopes that reach the catchment with precipitation, thus reflecting the water mixing, diversity of flow paths and their velocities (Kirchner, 2016a; McGuire and McDonnell, 2006).

Kirchner (2016a, b) proposed the young water fraction, i.e., the fraction of water in a stream younger than roughly 2-3 months. This young water fraction can be reliably estimated from the ratio between the amplitudes of the seasonal isotope cycles in streamwater and precipitation, respectively (Kirchner, 2016a). The precipitation isotope cycle amplitude (A_P) is estimated through a robust fit of a sine function on the isotopic composition of precipitation samples by using the precipitation amount associated to each sample as weight for reducing the influence of low-precipitation events (von Freyberg et al., 2018a; Kirchner, 2016a). Concurrently, streamwater isotope cycle amplitude is estimated through a robust fit of a sine function on the isotopic composition of streamwater samples with or without using discharge *(Q)* at the sampling time as weights (von Freyberg et al., 2018a). Therefore, it is necessary to distinguish between the unweighted and the flow-weighted streamwater amplitude (A_S and A^*_S, respectively) and, accordingly, between the time-weighted and the flow-weighted young water fraction (F_{yw} and F^*_{yw}, respectively). Please note that hereafter the symbol "*" indicates a streamflow-weighted variable.

Recently, Gallart et al. (2020b) proposed a new approach for estimating the sensitivity of young water fraction to stream discharge by fitting the following sinusoid function (Eq. 1) directly to the seasonal variation of the isotopic signal of stream water:

$$c_S(Q,t) = A_P\left[F^*_{yw}(Q)\right]\sin(2\pi f t - \varphi^*_S) + k^*_S = A_P[1-(1-F^*_0)\exp(-Q\,S^*_d)]\sin(2\pi f t - \varphi^*_S) + k^*_S \quad (1)$$

Where F^*_0, S^*_d, φ^*_S and k^*_S parameters are obtained through non-linear fitting. The S^*_d (d mm^{-1}) parameter is defined as the discharge sensitivity of young water fraction, F^*_0 (-) is the virtual young water fraction when Q = 0, φ^*_S (rad) is the phase of the seasonal cycle, f is the frequency (equal to 1 y^{-1} for a seasonal cycle) and k^*_S (‰) is a constant representing the vertical

https://doi.org/10.5194/egusphere-2023-1797
Preprint. Discussion started: 5 September 2023
© Author(s) 2023. CC BY 4.0 License.

offset of the seasonal cycle. As is evident from Eq. (1), the young water fraction is assumed to vary with discharge following an exponential-type equation that converges toward 1 at the highest flows (see supplementary material for additional methodological details), but which does not converge toward 0 at the lowest flows, thus theoretically admitting $F_0^* < 0$.

Because of this mathematical relationship between young water fraction and Q (see Eq. (6) in Gallart et al., 2020b), young water fraction time series can in theory be calculated at the same temporal resolution as Q. However, the uncertainties of such time series can be substantial because the underlying isotope data generally are not able to capture the entire range of flow regimes, especially the (very) high flow rates (Xia et al., 2023). This becomes evident in Figs. 1 and 3 of Gallart et al. (2020b) where standard errors of flow-specific F_{yw} are largest during the highest flows. From these considerations emerges the need for a new method to reliably estimate the time series of young water fractions, and to better constrain the discharge sensitivity of young water fractions at very low and very high flow conditions.

In this regard, we propose a new multi-tracer method which combines both stable water isotopes ($\delta^{18}O$) and the electrical conductivity (EC), which is a bulk measure of the major ions in water (Riazi et al., 2022). As a tracer, EC is advantageous because it can be measured over extended periods at high temporal resolution, while costs for installation and maintenance remain low (Cano-Paoli et al., 2019; Mosquera et al., 2018). However, EC is not an inert tracer because it is affected by geochemical reactions and dissolution of non-conservative solutes in streamwater (Cano-Paoli et al., 2019; Benettin et al., 2022). Stable water isotopes, on the other hand, are typically sampled at much lower temporal resolutions than EC because costs for sampling and laboratory analysis are much higher (Mosquera et al., 2018). Isotopes are considered conservative tracers that do not undergo chemical reactions. Because of these characteristics, the tracers EC and stable water isotopes complement each other well, and thus can be used to constrain model parametrizations and to inform transit time models (Cano-Paoli et al., 2019; Benettin et al., 2022). The main objective of this paper is to leverage high-resolution and low-cost EC measurements and bi-weekly $\delta^{18}O$ data to develop a method for reducing the uncertainty of discharge sensitivity of young water fraction and for estimating the young water fraction at higher temporal resolution.

2 Material and Methods

2.1 Study sites and data set

To test the applicability of our method (section 2.2), we use data from the Erlenbach (ERL), Lümpenenbach (LUE) and Vogelbach (VOG) catchments, located in the pre-Alpine Alptal valley in central Switzerland. The geographical framework of the three study sites is reported in Fig. 1.

https://doi.org/10.5194/egusphere-2023-1797
Preprint. Discussion started: 5 September 2023
© Author(s) 2023. CC BY 4.0 License.

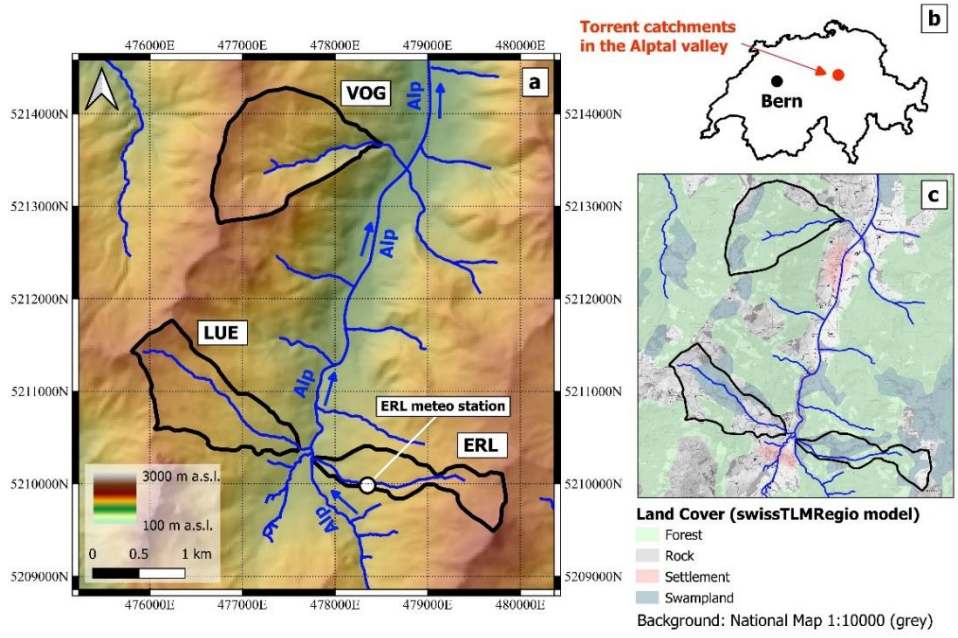

Figure 1 a) Location of the three study catchments with indication of the stream networks and elevation (DHM25 ©swisstopo) as background. The Alp river is marked in the map with blue arrows indicating its flow direction. b) Location of the Alptal valley in Switzerland. c) Land cover of the three study catchments from the ©swissTLMRegio 2D landscape model.

The three study catchments cover areas between 0.7 and 1.6 km^2, and mean elevation ranges from 1335 to 1359 m a.s.l (Table 1, Fig. 1a). Mean catchment slopes are 13.53°, 12.49° and 18.42° in the ERL, LUE and VOG catchments, respectively, but the hillslopes can be much steeper locally (20°-40°) (Stähli et al., 2021). According to the swissTLMRegio model (Fig. 1c), the ERL catchment is mainly constituted by forest (45%) and swampland (49%) which are the dominant classes also in the LUE (21% and 39%, respectively) and VOG (72% and 13%, respectively) catchments. Most of the southern Alptal valley is characterized by shallow gleysols with low permeability that limit the deep infiltration of water and lead to shallow groundwater tables (Stähli et al., 2021). The percentage of soils with low storage capacity is about 4% in both ERL and LUE, while it is 51% in the VOG catchment; a large fraction of the soils is saturated (≥ 95% in ERL and LUE, 49% in VOG; von Freyberg et al., 2018). The geological substratum of the three study sites consists mainly of sedimentary rock (flysch). The catchment area covered by Quaternary deposits is much higher in the ERL and LUE catchments than in the VOG catchment (Table 1). Therefore, although the study catchments are located within close proximity, they differ in terms of soil wetness and unconsolidated sediments.

The average hydro-climatic conditions are generally similar for all three catchments. The average annual precipitation in the period January 2000 - December 2015, based on interpolated data from the PREVAH model, was about 1853 mm, 1803 mm and 1800 mm at the ERL, LUE and VOG catchments, respectively (von Freyberg et al., 2018a). The average monthly discharge is similar among the catchments: it is 138.9, 152.0, and 117.4 mm month^{-1} at the ERL, LUE and

https://doi.org/10.5194/egusphere-2023-1797
Preprint. Discussion started: 5 September 2023
© Author(s) 2023. CC BY 4.0 License.

VOG catchments, respectively (von Freyberg et al., 2018a). These watersheds reveal an hybrid hydro-climatic regime (Staudinger et al., 2017; von Freyberg et al., 2018a), since we observe an ephemeral snowpack formation (typically from December to April) that also during winter rapidly melts away so that the snowpack may not last throughout the entire winter season (Stähli et al., 2021).

Daily resolution Q and streamwater EC data have been downloaded from the Swiss Federal Office for Forest, Snow and Landscape Research (WSL, Birmensdorf, Switzerland) data portal. We have estimated the Q-EC relationships with a log-type fit (Fig. 2). As daily Q increases, daily EC decreases in the three study sites. This pattern arises due to the contribution of different sources (i.e., ages) of water to the stream. At the three study sites, stream discharge increases due to rainfall or snowmelt, which are generally low in EC, resulting in a dilution of streamwater EC. In addition, during wet conditions (high Q), more rapid flow paths are activated leading to a prevalence of the younger hydrograph component. Because of the short interaction time with mineralized rocks and soils, young water can be assumed to be poor of dissolved ions (i.e., low EC). The other extreme, low Q and high streamwater EC, occurs during baseflow conditions when the stream is mainly fed by old (i.e., highly-mineralized, high-EC) subsurface water (Schmidt et al., 2012).

This study uses F_{yw}, F^*_{yw}, F^Q_{yw} and S^*_d (Table 2, Table 4), which were estimated in past studies (Gallart et al., 2020b; von Freyberg et al., 2018a) by considering streamflow $\delta^{18}O$ data from biweekly grab sampling over a period of approximately 5 years for the three study catchments. F^Q_{yw} values refer to young water fractions estimated by separating the streamwater isotope time series into different discharge ranges and calculating the seasonal isotope cycles (A^Q_S) values individually for each of these flow regimes (von Freyberg et al., 2018a). For more details about F^Q_{yw} estimation, the reader is referred to Kirchner (2016b) and von Freyberg et al. (2018a).

Table 1 Topographic, geological and hydro-climatic properties of the three study sites. Superscript "1" refers to data published in von Freyberg et al. (2018a); Superscript "2" refers to data published in Gentile et al. (2023).

Catchment ID	ERL	LUE	VOG
[1]Area (km^2)	0.7	0.9	1.6
[1]Mean elevation (range) (m a.s.l.)	1359 (1117–1650)	1336 (1092–1508)	1335 (1038–1540)
[2]Mean slope (°)	13.53	12.48	18.42
[1]Saturated soils (%)	0.95	0.96	0.49
[2]Geological substratum	Sed. Rock (flysch)	Sed. Rock (flysch)	Sed. Rock (flysch)
[2]Areal fraction of Quaternary deposits (-)	0.74	0.9	0.48
[1]Regime (Staudinger et al., 2017)	hybrid	hybrid	hybrid
[1]Average precipitation (mm/month)	162.4	157.1	162.2
[1]Average discharge (mm/month)	138.9	152	117.3
[1]Period of isotope sampling	Jul 2010- May 2015	Oct 2010-Nov 2015	Jun 2010-Nov 2015

https://doi.org/10.5194/egusphere-2023-1797
Preprint. Discussion started: 5 September 2023
© Author(s) 2023. CC BY 4.0 License.

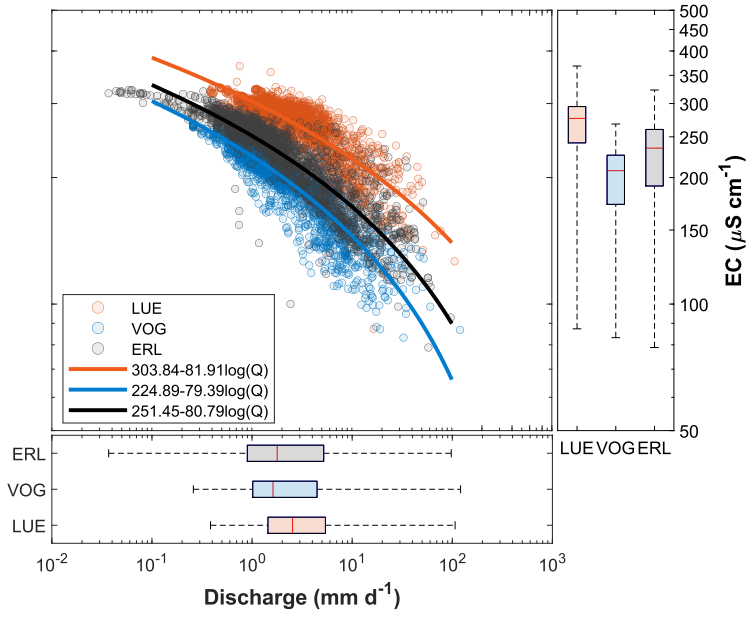

Figure 2 Relation between daily EC and daily *Q* for the three study sites. As discharge increases, the electrical conductivity (EC) decreases in the three study catchments. This pattern arises mainly due to the age (source) of water contributing to the stream: if a substantial amount of recent, low-EC water contributes to streamflow during rainfall or snowmelt, streamwater EC decreases while discharge increases.

Table 2 Young water fractions of distinct flow regimes (F^{Q}_{yw}), as well as average time-weighted (F_{yw}) and flow-weighted (F^{*}_{yw}) young water fractions with corresponding standard errors (SE). The number of samples used for estimating F^{Q}_{yw} and the median *Q* of each flow regime are also reported. These data were previously obtained by von Freyberg et al. (2018a).

Catch. ID	Q (range)	n° samples	Median Q (mm d^{-1})	$F^{Q}_{yw} \pm SE$	$F_{yw} \pm SE$	$F^{*}_{yw} \pm SE$
ERL	Q (0-25%)	35	0.42	0.294±0.039	0.37 ± 0.03	0.49 ± 0.03
	Q (25-50%)	35	0.93	0.353±0.032		
	Q (50-75%)	35	2.21	0.449±0.049		
	Q (75-100%)	35	7.23	0.467±0.048		
	Q (80%)	28	8.20	0.446±0.061		
	Q (90%)	14	19.21	0.52±0.083		
LUE	Q (0-25%)	33	1.11	0.189±0.024	0.25 ± 0.02	0.33 ± 0.03
	Q (25-50%)	33	1.81	0.205±0.029		
	Q (50-75%)	33	3.56	0.363±0.039		
	Q (75-100%)	33	7.68	0.356±0.051		
	Q (80%)	27	9.16	0.35±0.057		
	Q (90%)	14	12.59	0.403±0.075		
VOG	Q (0-25%)	35	0.73	0.163±0.02	0.21 ± 0.02	0.31 ± 0.02
	Q (25-50%)	35	1.11	0.168±0.024		

https://doi.org/10.5194/egusphere-2023-1797
Preprint. Discussion started: 5 September 2023
© Author(s) 2023. CC BY 4.0 License.

	Q (50-75%)	34	2.22	0.267±0.034		
	Q (75-100%)	35	7.80	0.316±0.039		
	Q (80%)	28	8.65	0.325±0.044		
	Q (90%)	14	12.13	0.36±0.051		

2.2 The *EXPECT* method: two-component *E*lectrical *C*onductivity-based hydrograph separa*T*ion employing an *EXP*onential mixing model

In the realm of catchment hydrology, the use of additional hydrochemistry data together with stable water isotopes can provide unprecedented insights into transit time research, hydrological processes, and the links between water quality and water age variations (Benettin et al., 2022, 2017). The multi-tracer method we present in this paper lays its foundations on the statement that the isotope-based F_{yw} and F^*_{yw}, Eq. (2.1) and Eq. (2.2), accurately estimate the time-weighted and the flow-weighted average young water fractions in streamflow, respectively (Kirchner, 2016b).

$$F_{yw} = \frac{A_S}{A_P} \tag{2.1}$$

$$F^*_{yw} = \frac{A^*_S}{A_P} \tag{2.2}$$

Accordingly, if we knew the young water fraction over a generic time step t_i, $F_{yw}(t_i)$ (e.g., daily young water fraction), we could calculate the time-weighted and the flow-weighted average young water fraction in streamflow through Eq. (3.1) and Eq. (3.2), respectively:

$$\tilde{F}_{yw} = \frac{\sum_{i=1}^{n} F_{yw}(t_i)}{n} \simeq F_{yw} \tag{3.1}$$

$$\tilde{F}^*_{yw} = \frac{\sum_{i=1}^{n} Q(t_i) F_{yw}(t_i)}{\sum_{i=1}^{n} Q(t_i)} \simeq F^*_{yw} \tag{3.2}$$

where n is the number of time-steps (e.g., days) in the period of isotope sampling and $Q(t_i)$ is the discharge at the time t_i (e.g., daily discharge). The hat "~" symbol is simply used to visually differentiate the average young water fractions obtained with both approaches. Please, note that Eq. (3.2) was previously presented in Gentile et al. (2023). The definition of the fraction of the streamflow younger than a threshold age (varying modestly from 2 to 3 months) at the generic time t_i, $F_{yw}(t_i)$, implicitly defines the existence of a complementary fraction of streamflow older than that threshold age at the same time t_i, $F_{ow}(t_i)$. Thus, mass conservation requires:

$$F_{yw}(t_i) + F_{ow}(t_i) = 1\,, \tag{4}$$

To estimate $F_{yw}(t_i)$, and thus $F_{ow}(t_i)$, we separate the hydrograph into young and old water by using EC as a tracer. A time-source separation is generally performed using isotope hydrograph separation, IHS, (Klaus and McDonnell, 2013), while major ions (approximated by EC) have been previously used for geographic-source separation in endmember mixing analysis (Hooper, 2003; Penna et al., 2017). Nevertheless, the choice to employ EC for a time-source separation is justified

https://doi.org/10.5194/egusphere-2023-1797
Preprint. Discussion started: 5 September 2023
© Author(s) 2023. CC BY 4.0 License.

here by considering that water from different sources within the catchment is likely to have different ages. Hence, EC can potentially provide useful information on water age (Riazi et al., 2022) because a longer residence time of a water parcel inside the catchment will likely result in increased solute concentration once it will be released as streamflow (Benettin et al., 2017).

To perform the hydrograph separation, we assume that streamwater EC at the generic time t_i, $EC_S(t_i)$, decreases exponentially with increasing young water contributions to streamflow:

$$EC_S(t_i) = EC_{ow} e^{-aF_{yw}(t_i)}\,, \tag{5}$$

where, EC_{ow} is the old water EC endmember and a is a parameter. The exponential decay proposed in Eq. (5) guarantees a realistic scenario for the case $F_{yw}(t_i) = 0$, i.e. streamflow contains only old water ($F_{ow}(t_i) = 1$) and streamwater EC is equal to EC_{ow} ($EC_S(t_i) = EC_{ow}$). Conversely, if $F_{yw}(t_i)$ is equal to 1, streamflow is made up entirely of young water. Accordingly, we can include the following condition: if $F_{yw}(t_i) = 1$, $EC_S(t_i) = EC_{yw}$ where EC_{yw} is the young water EC endmember (Eq. 6).

$$EC_{yw} = EC_{ow} e^{-a}\,, \tag{6}$$

Furthermore, we assume $EC_{yw} < EC_{ow}$ simply because old water had longer contact with mineral surfaces in the subsurface, and thus weathering-derived solute concentrations will be higher in old water compared to that in young water. By further considering the law of water mass conservation (Eq. 4), it is possible to solve the system of three equations (Eq. 4, 5, 6) with three variables ($a, F_{yw}(t_i), F_{ow}(t_i)$), thus obtaining the explicit expression of a (Eq. 7) and, accordingly, of $F_{yw}(t_i)$ (Eq. 8).

$$a = -\ln\left(\frac{EC_{yw}}{EC_{ow}}\right), \tag{7}$$

$$F_{yw}(t_i) = \frac{\ln\left(\frac{EC_S(t_i)}{EC_{ow}}\right)}{\ln\left(\frac{EC_{yw}}{EC_{ow}}\right)}, \tag{8}$$

Despite the relatively simple mathematical approach, the main difficulty in applying Eq. (8) to estimate $F_{yw}(t_i)$ is that we generally cannot accurately determine the endmembers EC_{yw} and EC_{ow} from measurements as they correspond to the (rare) scenarios in which $F_{yw}(t_i)$ is either 0 or 1. The first scenario ($F_{yw}(t_i) = 0$) might occur only after prolonged periods without rainfall or snowmelt while the second scenario ($F_{yw}(t_i) = 1$) is unlikely to occur in most natural catchments where baseflow is usually older than 3 months (Gentile et al., 2023), and thus we cannot directly measure EC_{yw} (Kirchner, 2016b). We therefore determine EC_{yw} and EC_{ow} through calibration, respecting the following three constraints:

i. EC_{ow} and EC_{yw} are greater than or equal to 0.
ii. $\tilde{F}_{yw}$, where $F_{yw}(t_i)$ is obtained through Eq. (8), must match the F_{yw} estimated with the amplitude ratio technique (Eq. 2.1).

https://doi.org/10.5194/egusphere-2023-1797
Preprint. Discussion started: 5 September 2023
© Author(s) 2023. CC BY 4.0 License.

iii. $\tilde{F}^*_{yw}$, where $F_{yw}(t_i)$ is obtained through Eq. (8), must match the F^*_{yw} estimated with the amplitude ratio technique (Eq. 2.2).

In summary, we perform a constrained EC-based hydrograph separation in which the two endmembers (EC_{yw} and EC_{ow}) are calibrated through an optimization procedure. Specifically, we use the © Matlab *fmincon* solver, the *sqp* (sequential quadratic programming) algorithm, within the *GlobalSearch* procedure that runs repeatedly the local solver for generating a global solution. To satisfy point i), we search the endmember values within the range [0, + ∞). We consider ∞ as upper limit since catchments can also have immobile storages that potentially will never participate to the water cycle (Staudinger et al., 2017). In addition, we calibrate the EC endmembers by minimizing the following objective function, which is designed for satisfying points ii) and iii).

$$obj = \frac{\left(\tilde{F}_{yw} - F_{yw}\right)^2 + \frac{F^*_{yw}}{F_{yw}}\left(\tilde{F}^*_{yw} - F^*_{yw}\right)^2}{\left(1 + \frac{F^*_{yw}}{F_{yw}}\right)}, \quad (9)$$

We are giving a greater weight to the second term, $\left(\tilde{F}^*_{yw} - F^*_{yw}\right)^2$. The weight is proportional to how much F^*_{yw} is higher than F_{yw}, since Gallart et al. (2020a) showed that the flow-weighted analysis produces a less biased estimation of young water fraction. The outputs of the optimization procedure are the calibrated young water and old water endmembers (EC^{opt}_{yw} and EC^{opt}_{ow}, respectively). Subsequently, we calculate the F^{opt}_{yw} (at every time step t_i) with Eq. (8) by using the optimal endmembers ($EC^{opt}_{yw}, EC^{opt}_{ow}$) and we plot F^{opt}_{yw} against Q, thus visualizing an empirical relationship between the two variables. Finally, we fit Eq. (6) from Gallart et al. (2020b) to our F^{opt}_{yw} data:

$$F^{opt}_{yw} = 1 - (1 - F^{EXP}_0)\exp(-Q\, S^{EXP}_d), \quad (10)$$

We then compare the discharge sensitivity, S^*_d, determined from streamwater isotope data, see Eq. (1), and the discharge sensitivity, S^{EXP}_d, determined from Eq. (10). We further compare our results to the F^Q_{yw} values (Table 2) previously obtained by von Freyberg et al. (2018a).

We apply our method at two different time-resolutions that are reflected in our data set. At daily resolution (DR), $EC_S(t_i)$ and $Q(t_i)$ refer to daily average EC and Q, respectively, and thus, $F_{yw}(t_i)$ is the average young water fraction of each day. Analogously, at sampling resolution (SR), $EC_S(t_i)$ and $Q(t_i)$ correspond to the daily-average EC and Q values recorded approximately every 2 weeks (i.e., at the date of isotope streamwater grab sampling), respectively. At SR, $F_{yw}(t_i)$ values are estimated only for those days on which an isotope sample was taken.

Last, but not least, since our method consists in a two-component *E*lectrical *C*onductivity-based hydrograph separa*T*ion employing an *EXP*onential mixing model, we decide to name it *EXPECT*. A schematic representation of the *EXPECT* method is reported in Fig. 3.

https://doi.org/10.5194/egusphere-2023-1797
Preprint. Discussion started: 5 September 2023
© Author(s) 2023. CC BY 4.0 License.

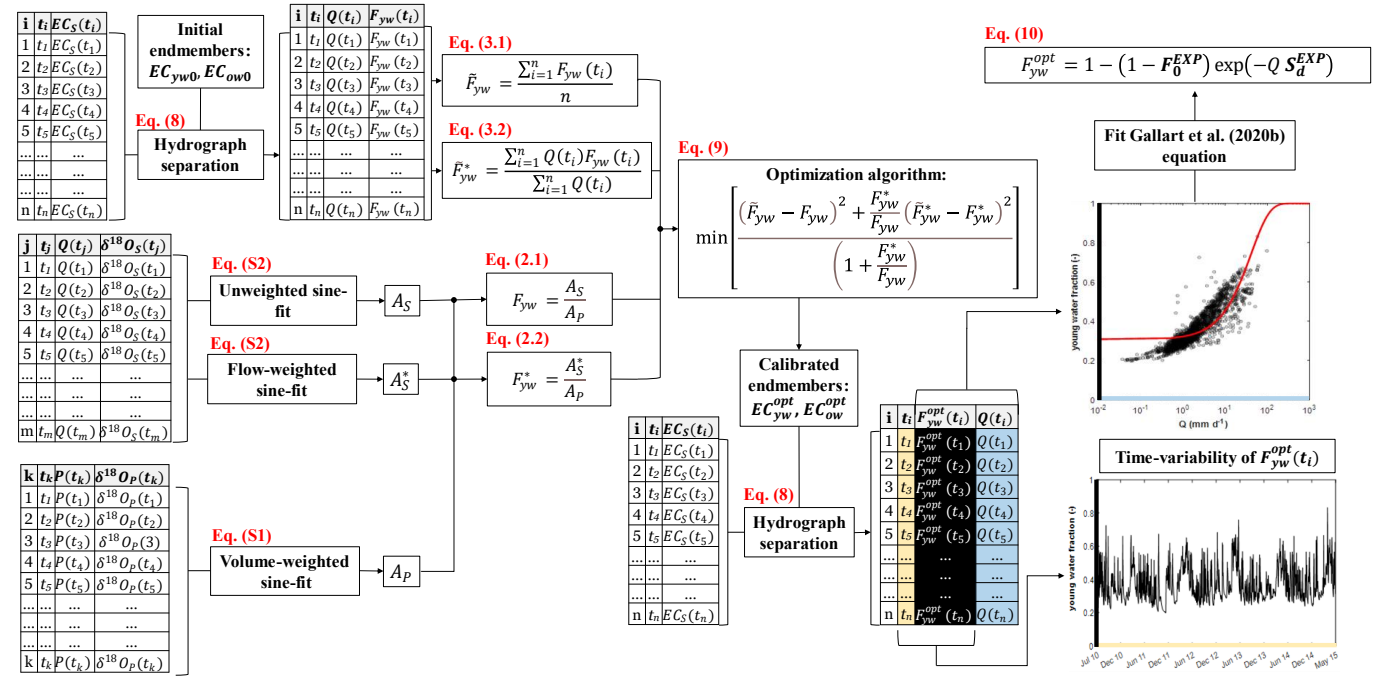

Figure 3 Schematic representation of the *EXPECT* method. The subscript "P" refers to precipitation, while the subscript "S" refers to streamwater. $P(t_k)$ indicates the volume of precipitation used for the volume-weighted fit of precipitation isotopes ($\delta^{18}O_p(t_k)$). The sampling times of $EC_S(t_i)$, $Q(t_i)$, $\delta^{18}O_S(t_j)$, $\delta^{18}O_P(t_k)$ are generally not the same, and thus the times t_i, t_j and t_k have different indices.

We quantify the uncertainty of EC^{opt}_{yw} and EC^{opt}_{ow} by repeating the global optimization procedure by sampling randomly 10000 couples of F_{yw} and F^*_{yw} from the intervals F_{yw} ± SE and F^*_{yw} ± SE, respectively. The SE values are reported in Table 2. The random sampling assumes that the values within the two intervals have a Gaussian probability of extraction, thus favoring the sampling of the core values. Therefore, we obtain 10000 couples of endmembers of which we compute statistics. We further calculate the uncertainty of $F^{opt}_{yw}(t_i)$: we apply Eq. (8) using the 10000 couples of endmembers, thus obtaining 10000 $F^{opt}_{yw}(t_i)$ values at each time step t_i, of which we calculate the standard deviation.

Please, note that the initial conceptualization of the *EXPECT* method was based on testing the hydrograph separation by using the widely established 2-component endmember linear mixing approach (Buttle, 1994; Genereux, 1998; Klaus and McDonnell, 2013). However, this approach was not successful because it can represent only a limited hydrological behaviour of catchments that does not capture that of our three study catchments. A detailed explanation of the limits regarding the linear mixing model is provided in the appendix A of this paper.

https://doi.org/10.5194/egusphere-2023-1797
Preprint. Discussion started: 5 September 2023
© Author(s) 2023. CC BY 4.0 License.

3 Results and Discussion

3.1 Physical likelihood of calibrated endmembers and discharge sensitivity of young water fraction

The application of the *EXPECT* method showed, at both daily and sampling resolution, that the old water EC endmembers, EC_{ow}^{opt} are about one order of magnitude larger than the young water EC endmembers EC_{yw}^{opt} for all three experimental catchments (Table 3, Fig. 4). The highest EC_{ow}^{opt} values were obtained for ERL (501 $\mu S\ cm^{-1}$, DR), and the lowest values in VOG (319 $\mu S\ cm^{-1}$, DR). The EC_{ow}^{opt} values are in line with those measured in groundwater: in a 6.8-m deep monitoring well at the ERL meteorological station, groundwater EC varies generally between 400 (spring-summer) and 500 $\mu S\ cm^{-1}$ (fall-winter; data not shown), whereas in a neighbouring catchment of ERL, EC in groundwater in up to 1.5 m depth was generally around 400-450 $\mu S\ cm^{-1}$ during no-snowmelt conditions (Kiewiet et al., 2020). Fig. 4 shows further that the interquartile ranges of the EC_{ow}^{opt} empirical distributions are much larger than those of EC_{yw}^{opt}. Assuming that the solute concentration in streamwater increases with water age (Riazi et al., 2022), this can possibly be explained with the much wider range of transit times (from approximately 0.2 to ∞ y) of the old water compared to that of young water (0 to 0.2 y). Consequently, the concentrations of weathering-derived solutes are not only higher but also more variable than in young water.

Our method estimates the EC endmember values for the cases $F_{yw}(t_i) = 1$ and $F_{yw}(t_i) = 0$ that are generally difficult to determine experimentally, thus providing additional information about young and old water in the system under study. In this regard, in each one of the three study sites, the theoretical endmembers EC_{yw}^{opt} are lower than the minimum EC value measured in the streams; analogously, the calibrated EC_{ow}^{opt} values are higher than the maximum measured EC value (boxplots *versus* horizontal dashed lines in Fig. 4). This is expected for a natural, heterogeneous system where incoming precipitation mixes with stored water, and thus streamwater never contains 100% young or old water, respectively. Instead, streamwater is a mixture of these two components that, depending on catchment wetness conditions and hydroclimatic forcing, contribute in different proportions to catchment outflow.

Table 3 Optimized endmembers obtained through the *EXPECT* method. 1st, 2nd, 3rd quartile (q_1, q_2 and q_3, respectively) and IQR of endmembers empirical distribution are also reported. Values are in $\mu S\ cm^{-1}$.

Time-resolution	Catchment	EC_{yw}^{opt}	q_1	q_2	q_3	IQR	EC_{ow}^{opt}	q_1	q_2	q_3	IQR
Daily (DR)	ERL	54.25	44.28	54.05	63.17	18.89	501.03	446.52	502.47	583.37	136.85
	LUE	51.08	37.27	50.67	65.02	27.75	449.79	411.12	450.29	504.31	93.19
	VOG	29.71	23.79	29.45	35.13	11.34	318.82	300.33	319.92	345.73	45.4
Sampling (SR)	ERL	44.78	35.88	44.74	53.4	17.52	565.89	495.15	566.39	668.09	172.94
	LUE	65.68	49.29	65.18	80.93	31.64	410.43	379.38	410.69	454.26	74.88
	VOG	32.25	25.64	31.41	37.27	11.63	315.23	299.56	318.53	342.67	43.11

https://doi.org/10.5194/egusphere-2023-1797
Preprint. Discussion started: 5 September 2023
© Author(s) 2023. CC BY 4.0 License.

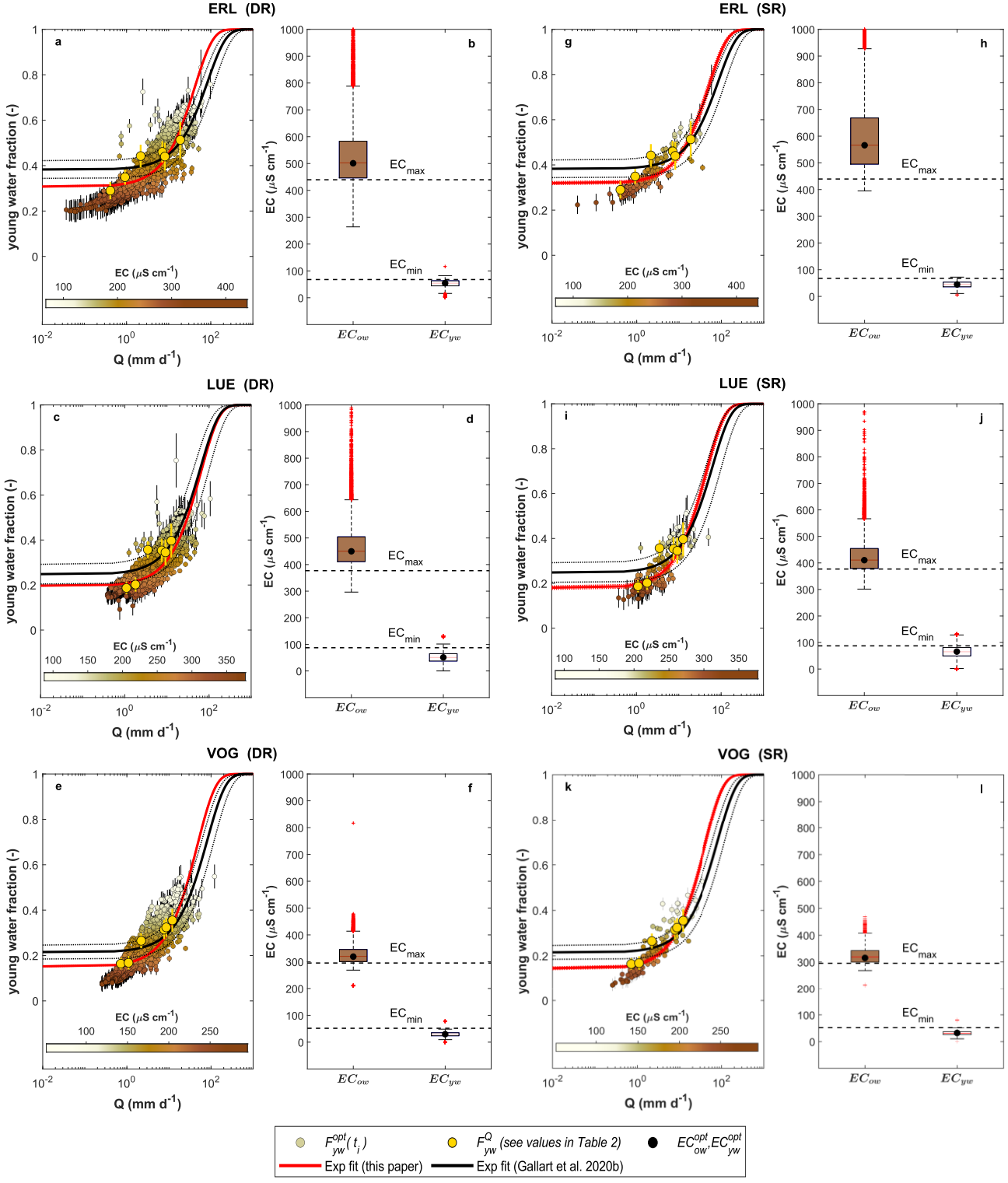

https://doi.org/10.5194/egusphere-2023-1797
Preprint. Discussion started: 5 September 2023
© Author(s) 2023. CC BY 4.0 License.

Figure 4 $F_{yw}^{opt}(t_i)$- $Q(t_i)$ relation for the ERL, LUE and VOG study catchments at daily resolution (DR, panels a, c, e) and sampling resolution (SR, panels g, i, k), as well as the corresponding EC endmembers (b, d, f and h, j, l, respectively). The white-brown colour of the $F_{yw}^{opt}(t_i)$ points indicates the $EC_S(t_i)$ value. For comparison, average F^{Q}_{yw}-values of specific flow ranges (Table 2) are shown in yellow. The black curve represents the exponential-type fit by using parameters S_d^* and F_0^* previously obtained through non-linear fitting of Eq. (1) to streamwater isotope data by Gallart et al. (2020b). The red curve represents the exponential-type fit by using parameters S_d^{EXP} and F_0^{EXP} obtained in this study through non-linear fitting of Eq. (10) to $F_{yw}^{opt}(t_i)$. Black and red dashed lines indicate ±1 standard error. Panels b), d), f), h), j), l) show the boxplots of EC_{yw}^{opt} and EC_{ow}^{opt} derived from the endmember uncertainty analysis. The black dots indicate the optimal endmembers (obtained constraining the *EXPECT* method using F_{yw} and F^*_{yw}) used to calculate $F_{yw}^{opt}(t_i)$ through Eq. (8). The dashed black lines, labelled with EC_{max} and EC_{min}, refer to the maximum and minimum EC values measured in the stream.

The estimated discharge sensitivity of the young water fraction, S_d^{EXP}, based on the *EXPECT* method satisfactorily describes the $F_{yw}^{opt}(t_i)$- $Q(t_i)$ relationships of the three catchments, as reflected by R^2 values of 0.58 and higher (Table 4; red curves in Figure 4). Moreover, the red curve also fits well the F^{Q}_{yw} values of the distinct flow regimes (Table 2). By taking advantage of the consecutive $F_{yw}^{opt}(t_i)$ values at daily or sampling resolution, we better constrain the parameters of Eq. (10) at very low and very high discharges compared to the fit obtained with Eq. (1) that is using only streamwater $\delta^{18}O$ data at sampling resolution (black curve in Figure 4, Table 4; see the supplement for methodological details). As a result, our estimated discharge sensitivity S_d^{EXP} is higher for the ERL and VOG catchments and similar (within error) for the LUE catchment compared to S_d^*, whereas our estimates of F_0^{EXP} for all three sites are slightly smaller than the respective F_0^* values obtained with Eq. (1).

We also find that the S_d^{EXP} values obtained at SR can differ from those at DR. For LUE, S_d^{EXP} at SR is larger than at DR (Table 4), whereas it is the other way around for ERL. Such differences can be attributed to the different flow regimes represented by the isotope samples that influences the EC endmember estimations at each site (Table 3). Moreover, at DR we are calibrating the EC endmembers by using F_{yw} and F^*_{yw} based on isotope data at SR. To be fully consistent in terms of temporal resolution, we theoretically need daily streamwater isotope data to derive F_{yw} and F^*_{yw}. The influence of sampling frequency is one of the limitations of the *EXPECT* method as explained in section 3.3. Nevertheless, the F_0^{EXP} values are consistent between the two temporal resolutions.

As can be seen in Fig. 4, the $F_{yw}^{opt}(t_i)$ values obtained with the EXPECT method form a data cloud around the idealized discharge sensitivity function of Eq. (10). Specifically, for a given discharge value, we obtain various $F_{yw}^{opt}(t_i)$ values, which can be explained by the delayed response of old water during precipitation events: while the young water fraction is generally highest during the rising limb of the hydrograph, it decreases during the falling limb when old water reaches the stream (von Freyberg et al., 2018b)

https://doi.org/10.5194/egusphere-2023-1797
Preprint. Discussion started: 5 September 2023
© Author(s) 2023. CC BY 4.0 License.

Table 4 Comparison of discharge sensitivity parameters obtained with the *EXPECT* method (S_d^{EXP}, F_0^{EXP}), by fitting Eq. (10) on $F_{yw}^{opt}(t_i)$ data (the goodness of fit is indicated by R^2), and parameters (S_d^*, F^*_0) by fitting Eq. (1) directly to the seasonal variation of the isotopic signal of stream water.

Time-resolution	Catch. ID	F^*_0±SE (-)	F_0^{EXP}±SE (-)	S_d^*±SE (d mm^{-1})	S_d^{EXP}±SE (d mm^{-1})	R^2
		Eq. (1), (Gallart et al., 2020b)	Eq. (10), this study	Eq. (1), (Gallart et al., 2020b)	Eq. (10), this study	this study
Daily (DR)	ERL	-	0.3047±0.002	-	0.024±0.0005	0.62
	LUE	-	0.1948±0.0016	-	0.0155±0.0003	0.61
	VOG	-	0.1488±0.0016	-	0.0211±0.0004	0.64
Sampling (SR)	ERL	0.382±0.0387	0.317±0.0062	0.012±0.0034	0.0198±0.0016	0.64
	LUE	0.246±0.0429	0.1773±0.0073	0.016±0.0056	0.0223±0.0017	0.58
	VOG	0.214±0.03	0.1415±0.0056	0.012±0.0036	0.0252±0.0015	0.70

3.2 An immediate application of the *EXPECT* method: flow duration curves of young/old water and the temporal variability of young water fractions.

Because the *EXPECT* method allows for estimating young water fractions $F_{yw}^{opt}(t_i)$ at up to daily resolution, we can determine the flow duration curves of young and old water discharge, respectively. Moreover, we calculate $Q_{50/50}$, i.e., the median discharge value at which 50 ± 1% of both young and old water exist in streamflow. In the ERL catchment, Fig. 5a shows that a shift from old-water dominated towards young-water dominated streamflow occurs for discharges larger than approximately 7.7 mm d^{-1} ($Q_{50/50}$; Fig. 5a). In the LUE and VOG catchments, the streamflow contains more old water than young water for most of the flow regime (Fig. 5b, Fig. 5c); only for relatively few occasions, when Q exceeds $Q_{50/50}$ (23.2 and 17.5 mm d^{-1}, respectively), the relative contribution of young water was slightly larger than that of old water.

By comparing $Q_{50/50}$ with the median stream discharge (Q_{med}), we observe that in all three study catchments $Q_{50/50}$ is higher than Q_{med} (Fig. 5). This result suggests that more than 50% of the time a major proportion of old water reaches the stream. In both the LUE and VOG catchments, $Q_{50/50}$ is higher than in the ERL catchment, revealing that the LUE and VOG streams are longer dominated by old water than the ERL stream. This explains why the isotope-based average young water fraction is higher in the ERL than in the LUE and VOG catchments (Table 2).

With the *EXPECT* method, the time-variability of $F_{yw}^{opt}(t_i)$ can be explored in detail, e.g. through comparing time series of $F_{yw}^{opt}(t_i)$ with those of other hydro-climatic variables (Fig. 6). Accordingly, we show hereafter a comparison between $F_{yw}^{opt}(t_i)$ and hydro-climatic observations at daily resolution of the ERL catchment since it has the most complete hydro-climatic data set (including discharge, precipitation, snow depth and temperature measurements; all data available from WSL) compared to the other two catchments. As visible from Fig. 6, daily young water fractions in the ERL catchment respond directly to precipitation events, which is further reflected by a strong positive correlation between $F_{yw}^{opt}(t_i)$ and the

https://doi.org/10.5194/egusphere-2023-1797
Preprint. Discussion started: 5 September 2023
© Author(s) 2023. CC BY 4.0 License.

daily precipitation volumes ($\rho_{Spearman}$ = 0.41, p-value << 0.01 considering only days with precipitation, Fig. 7). We estimate that after a rainfall- or snowmelt event, the growth rate of $F_{yw}^{opt}(t_i)$ is on average 0.062±0.058 d^{-1} (to reach the local $F_{yw}^{opt}(t_i)$ maximum next to the previous $F_{yw}^{opt}(t_i)$ local minimum, Fig. S1). On the other side, during the recession phase, the average rate of decrease of $F_{yw}^{opt}(t_i)$ is -0.041±0.036 d^{-1} (to reach the $F_{yw}^{opt}(t_i)$ local minimum next to the previous $F_{yw}^{opt}(t_i)$ local maximum, Fig. S1). Accordingly, $F_{yw}^{opt}(t_i)$ rapidly increases after an event (peak $F_{yw}^{opt}(t_i)$ is reached on average after 1.98±1.25 days), while it recedes slower during no-input days (the next minimum $F_{yw}^{opt}(t_i)$ is reached on average after 3.36±3.10 days). The largest daily young water fractions in the ERL catchment occurred during spring snow melt (March-May), suggesting that the melt water of the ephemeral snowpack is an important source of young water (since no relevant water aging is observed in such snowpack) that flows off quickly in the stream (Gentile et al., 2023). Rapid surface runoff of snow melt can occur due to soil freezing (temperatures < 0°C) or high soil moisture contents (temperatures > 0°) both of which can limit infiltration (Harrison et al., 2021; Keller et al., 2017; Fig. 6). During the periods of snow accumulation and persistent snow cover, typically from November to February, $F_{yw}^{opt}(t_i)$ values were often as low as 0.3 and did not vary much (except during snowmelt and rain-on-snow events). Thus, streamflow in ERL was mainly composed of old water during this period, likely originating from the soil- and groundwater storages.

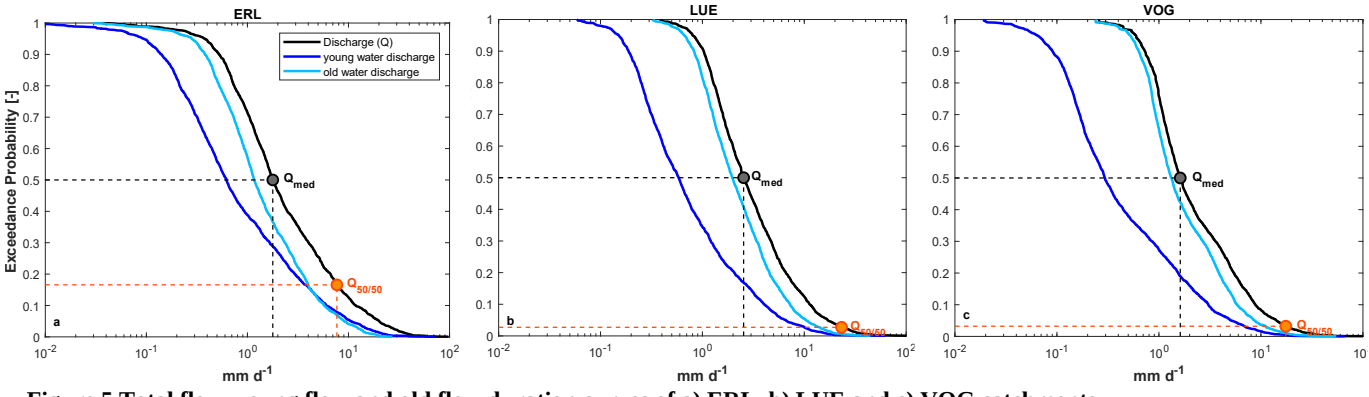

Figure 5 Total flow, young flow and old flow duration curves of a) ERL, b) LUE and c) VOG catchments.

https://doi.org/10.5194/egusphere-2023-1797
Preprint. Discussion started: 5 September 2023
© Author(s) 2023. CC BY 4.0 License.

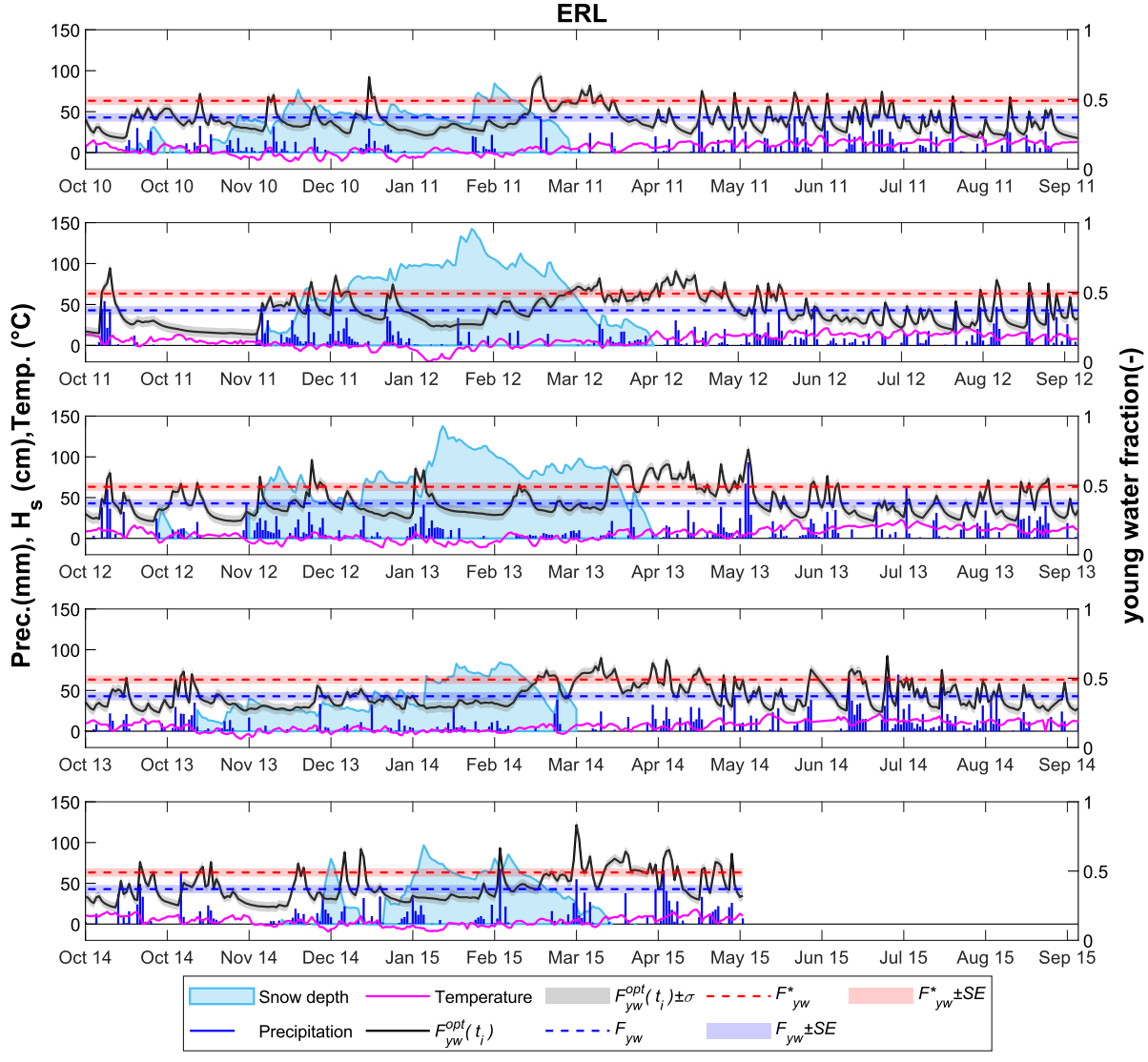

Figure 6 Time series of daily precipitation, snow depth, air temperature and F_{yw}^{opt} for the ERL catchment. Each panel reports a different hydrologic year.

https://doi.org/10.5194/egusphere-2023-1797
Preprint. Discussion started: 5 September 2023
© Author(s) 2023. CC BY 4.0 License.

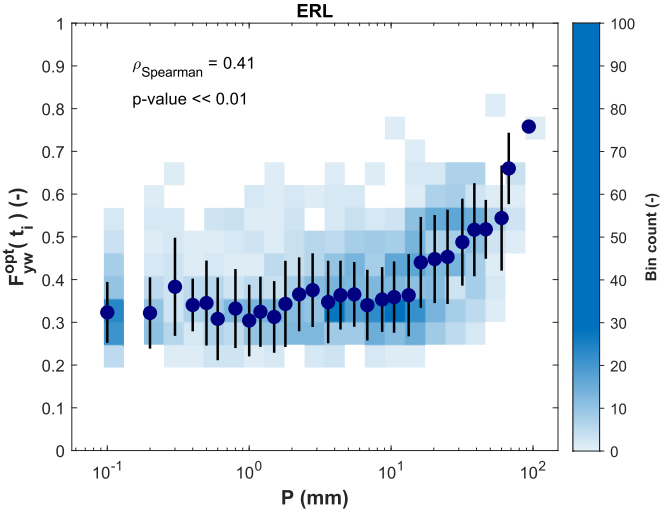

Figure 7 Correlation between daily F^{opt}_{yw} and daily precipitation when precipitation is higher than 0. Blue points indicate the median F^{opt}_{yw} observed in the stream corresponding to different ranges of daily precipitation with error bars indicating the standard deviation. These median F^{opt}_{yw} are plotted against the median daily precipitation in each range. The blue intensity of the bins indicates the number of observations within each bin. A rapid increase in young water fraction is observed when the daily precipitation is about 10 mm/d, thus reflecting hydrological connectivity and the generation of rapid flow paths.

3.3 Limitations of the *EXPECT* method

While the *EXPECT* method can offer valuable insights into the young water fraction's discharge sensitivity and its time-variability, it is not without its limitations. The assumption of considering EC as a proxy of streamwater age may not hold true in all hydrological systems. For example, human activities, such as mining, irrigation or waste water inputs can alter the streamwater EC in unpredictable ways. Another example involves catchments with highly soluble rocks in the aquifers (e.g., limestone or gypsum), that are susceptible to dissolution by water. It has been shown that EC can increase with Q in some karst systems due to remobilization of the circulating water in the fractured areas (Balestra et al., 2022). Therefore, the F_{yw}-EC relationship (Eq. 5) can be very different from that in our three study catchments that are mainly groundwater influenced.

Another major limitation of the *EXPECT* method is its strong dependency on reliable F_{yw} and F^*_{yw} estimates (i.e., assumptions ii) and iii) in section 2.2). If streamwater isotope data are short or sparse, F_{yw} or F^*_{yw} can be highly uncertain and the EC endmembers cannot be constrained sufficiently well. Recently, Gallart et al. (2020a) revealed that by using a weekly sampling frequency, time-weighted and flow-weighted young water fractions were significantly lower than results with virtual (perfect) sampling. Thus, for the same catchment, we could potentially obtain different EC endmembers if stable water isotopes were sampled at higher or lower temporal resolution.

For many catchments, Q and EC values are measured at sub-hourly resolution. Thus, theoretically the *EXPECT* method could provide reasonable young water fraction estimates results at these resolutions as well. However, we should consider

https://doi.org/10.5194/egusphere-2023-1797
Preprint. Discussion started: 5 September 2023
© Author(s) 2023. CC BY 4.0 License.

that short-term variations in EC may not necessarily represent short-term variations in water age. For example, Calles (1982) showed for a small stream in Sweden that diurnal variations in EC seem to be due to evapotranspiration, but also the influence from gravity variations may play a role. Moreover, a past study in a pre-alpine river in Switzerland revealed that diurnal fluctuation of EC can be due to biogeochemical processes, such as calcite precipitation and photosynthesis (Hayashi et al., 2012). Accordingly, the biological (photosynthesis and respiration) and chemical processes (carbonate equilibrium and calcite precipitation) can play a key role in controlling Ca^{2+} and HCO^{-}_{3} concentrations and, consequently, EC (Nimick et al., 2011; Hayashi et al., 2012). By calculating the average daily EC, thus removing diurnal and nocturnal EC dynamics, it should better reflect variations in water age under the *EXPECT* method assumptions.

Finally, we have chosen here an exponential mixing model (because we have shown that the linear mixing model is inconsistent with our observations, see appendix A) but the choice of the mixing model depends on the catchment properties.

4 Summary and Conclusions

The discharge sensitivity of the young water fraction (S^{*}_{d}) is a useful metric that quantifies how much the proportion of streamflow younger than 2–3 months changes as catchment wetness increases. In a past study, S^{*}_{d} was obtained by fitting a sine-function to the streamwater isotope values, assuming an exponential relationship between young water fraction and discharge (Gallart et al., 2020b). Most available streamwater isotope datasets are characterized by a relatively low sampling frequency, which often fail to capture the entire flow regime from very low to very high discharges. This can result in highly uncertain or unrealistic estimates of the discharge sensitivity of young water fractions. Therefore, this paper aims at incorporating EC and $\delta^{18}O$ data to develop a new method that a) estimates young water fractions at high temporal resolution by taking advantage of continuous EC measurements, and that b) better constrains the estimated discharge sensitivity.

We have designed the *EXPECT* method which combines two widespread techniques: the EC-based hydrograph separation and the sine-wave models of the seasonal isotope cycles. The method consists of a data-driven approach where the daily or biweekly (sampling) young water fractions are estimated directly from EC measurements considered as a proxy of the water age. Specifically, we use an exponential mixing model in which EC endmembers are calibrated by using time-weighted and flow-weighted young water fractions obtained from $\delta^{18}O$ data. The *EXPECT* method was tested in three small experimental catchments in Switzerland.

The application of this multi-tracer method has revealed that the optimal EC endmembers lie beyond the range of measured EC in streamwater. This result reflects that streams are commonly a mixture of young and old water and that corresponding EC endmembers are difficult to be obtained experimentally. The discharge sensitivities of the young water fractions for the three study sites, obtained with the *EXPECT* method, agree well with those obtained with the conventional approach that uses only isotope data. However, the *EXPECT* method significantly reduced the uncertainty of S^{*}_{d}. In addition, the method allows for estimating young water fractions at daily resolution, which provides interesting insights into short-term variations of streamwater age with changes in meteorological conditions, e.g., during snow accumulation and

https://doi.org/10.5194/egusphere-2023-1797
Preprint. Discussion started: 5 September 2023
© Author(s) 2023. CC BY 4.0 License.

snowmelt. Young water fractions at biweekly (i.e., sampling) resolution also revealed high reliability, thus highlighting the general applicability of this method also in ungauged catchments: $\delta^{18}O$ and EC data can be both obtained from laboratory analysis of collected water samples while *Q* can be directly measured in the stream with conventional methods (e.g., current meter method, weir method) without the presence of fixed instrumentation for measuring stream discharge and electrical conductivity.

To conclude, a recent review paper (Benettin et al., 2022) highlighted the challenge of integrating non-conservative tracers in lumped models, and thus explaining the lack of multi-tracer studies in the scientific literature. The *EXPECT* method is a first attempt to leverage the ease of EC data acquisition with stable water isotope data to improve the time resolution of young water fraction estimates. This method can (theoretically) be used to better constrain hydrological models that aim at determining water ages or to obtain new insights into hysteresis patterns of the relationships between young water fractions and discharge.

Appendix A: Limitations of the linear mixing model

In order to use EC to separate the hydrograph into young and old water at a specified time t_i, we may employ the 2-component EC-based Hydrograph Separation (ECHS), built on the water (Eq. A1) and tracer (Eq. A2) mass balance:

$$F_{yw}(t_i) + F_{ow}(t_i) = 1\,, \tag{A1}$$

$$EC_S(t_i) = EC_{yw}F_{yw}(t_i) + EC_{ow}F_{ow}(t_i)\,, \tag{A2}$$

Where, $EC_S(t_i)$ is the electrical conductivity measured in the stream at the time t_i, EC_{yw} is the young water EC endmember, EC_{ow} is the old water EC endmember. By solving the system of two equations (Eq. A1 and Eq. A2) with two variables ($F_{yw}(t_i)$ and $F_{ow}(t_i)$), we can obtain the explicit expression of $F_{yw}(t_i)$:

$$F_{yw}(t_i) = \frac{EC_S(t_i) - EC_{ow}}{EC_{yw} - EC_{ow}}\,, \tag{A3}$$

As mentioned in section 2.2, we assume $EC_{yw} < EC_{ow}$. However, by performing the constrained ECHS (section 2.2) in which the two endmembers (EC_{yw} and EC_{ow}) are calibrated, the optimization algorithm finds $EC_{yw} = 0$, that is exactly the lower bound of the defined range $[0, +\infty)$ in which the optimization algorithm searches the solution. This result suggests that the algorithm wants to search the best solution below the lower bound of the specified range, thus potentially returning a negative EC_{yw} value. Obviously, this mathematical solution is not physically acceptable, but we can investigate this result to better understand the catchment functioning. Accordingly, if we make explicit $EC_S(t_i)$ from Eq. (A3), we find a linear decrement of $EC_S(t_i)$ with the increasing $F_{yw}(t_i)$ (Eq. A4):

$$EC_S(t_i) = \left(EC_{yw} - EC_{ow}\right)F_{yw}(t_i) + EC_{ow} = \alpha\, F_{yw}(t_i) + EC_{ow}\,, \tag{A4}$$

https://doi.org/10.5194/egusphere-2023-1797
Preprint. Discussion started: 5 September 2023
© Author(s) 2023. CC BY 4.0 License.

By requiring a negative EC_{yw} as best solution, the constrained ECHS suggests that, for an exhaustive description of the catchments behaviour, $EC_S(t_i)$ needs to rapidly decrease at low $F_{yw}(t_i)$, as shown by the red lines in Fig. 8a. Nevertheless, physical reasons limit the slope (α) of this line (α ≥ -EC_{ow}); the most extreme, but still acceptable condition (i.e., when EC_{yw} = 0 and α = -EC_{ow}) is indicated by the dashed black line in Fig. 8a. Accordingly, to obtain a rapid decrease of $EC_S(t_i)$ at low $F_{yw}(t_i)$, but maintaining positive EC_{yw}, it is necessary to improve the linear mixing model. As visible from Fig. 8b, the exponential mixing model described in section 2.2 resulted suitable to describe a rapid decrease of $EC_S(t_i)$ at low $F_{yw}(t_i)$ by maintaining a positive EC_{yw}.

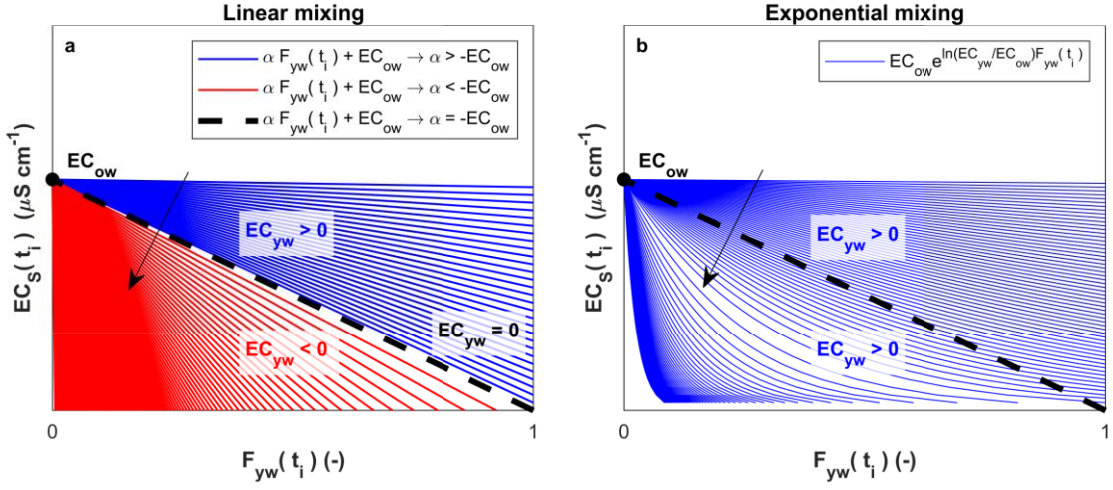

Figure 8 a) Limits of the linear decay of $EC_S(t_i)$ with increasing $F_{yw}(t_i)$. Red lines with slope (α) lower than -EC_{ow} are not physically admitted since they imply a negative EC_{yw}; b) the exponential mixing overcomes this limit. Black arrows indicate the direction in which EC_{yw} decreases.

Data availability. Time series of $\delta^{18}O$ in streamflow and precipitation for the ERL, LUE and VOG catchments are available in the data repository Zenodo at https://zenodo.org/record/4057967#.Y00oMHZBxPY (Staudinger et al., 2020). Daily discharge and electrical conductivity data for the ERL, LUE and VOG catchments are available from the *Swiss Federal Institute for Forest, Snow and Landscape research* (*WSL*) data portal at https://www.envidat.ch/#/metadata/longterm-hydrological-observatory-alptal-central-switzerland . The shape files (.shp) of the ERL, LUE and VOG catchments are available at https://zenodo.org/record/4057967#.Y00oMHZBxPY (Staudinger et al., 2020).

Author contributions. AG, JvF, and SF identified the research gap, designed the *EXPECT* method and prepared the paper. AG implemented the *EXPECT* method in a Matlab code with the support of DG and DC. All authors revised the manuscript and gave final approval to the submitted version.

https://doi.org/10.5194/egusphere-2023-1797
Preprint. Discussion started: 5 September 2023
© Author(s) 2023. CC BY 4.0 License.

Competing interests. The authors declare that they have no conflict of interest.

Acknowledgements. This work was supported by the "*PRIN MIUR 2017SL7ABC_005 WATZON Project*" and by *"Funding 2021 Fondazione CRT*". This publication is part of the project NODES which has received funding from the MUR –M4C2 1.5 of PNRR with grant agreement no. ECS00000036. Jana von Freyberg was supported by the Swiss National Science Foundation SNSF (grant PR00P2_185931). The results of this study have been discussed within the COST Action "WATSON", CA19120, supported by COST (European Cooperation in Science and Technology).

References

Balestra, V., Fiorucci, A., and Vigna, B.: Study of the Trends of Chemical–Physical Parameters in Different Karst Aquifers: Some Examples from Italian Alps, Water, 14, 441, https://doi.org/10.3390/w14030441, 2022.

Benettin, P., Bailey, S. W., Rinaldo, A., Likens, G. E., McGuire, K. J., and Botter, G.: Young runoff fractions control streamwater age and solute concentration dynamics, Hydrol. Process., 31, 2982–2986, https://doi.org/10.1002/hyp.11243, 2017.

Benettin, P., Rodriguez, N. B., Sprenger, M., Kim, M., Klaus, J., Harman, C. J., van der Velde, Y., Hrachowitz, M., Botter, G., McGuire, K. J., Kirchner, J. W., Rinaldo, A., and McDonnell, J. J.: Transit Time Estimation in Catchments: Recent Developments and Future Directions, Water Resour. Res., 58, e2022WR033096, https://doi.org/10.1029/2022WR033096, 2022.

Buttle, J. M.: Isotope hydrograph separations and rapid delivery of pre-event water from drainage basins, Prog. Phys. Geogr. Earth Environ., 18, 16–41, https://doi.org/10.1177/030913339401800102, 1994.

Calles, U. M.: Diurnal Variations in Electrical Conductivity of Water in a Small Stream, Hydrol. Res., 13, 157–164, https://doi.org/10.2166/nh.1982.0013, 1982.

Cano-Paoli, K., Chiogna, G., and Bellin, A.: Convenient use of electrical conductivity measurements to investigate hydrological processes in Alpine headwaters, Sci. Total Environ., 685, 37–49, https://doi.org/10.1016/j.scitotenv.2019.05.166, 2019.

Dansgaard, W.: Stable isotopes in precipitation, Tellus, 16, 436–468, https://doi.org/10.3402/tellusa.v16i4.8993, 1964.

von Freyberg, J., Allen, S. T., Seeger, S., Weiler, M., and Kirchner, J. W.: Sensitivity of young water fractions to hydro-climatic forcing and landscape properties across 22 Swiss catchments, Hydrol. Earth Syst. Sci., 22, 3841–3861, https://doi.org/10.5194/hess-22-3841-2018, 2018a.

von Freyberg, J., Studer, B., Rinderer, M., and Kirchner, J. W.: Studying catchment storm response using event- and pre-event-water volumes as fractions of precipitation rather than discharge, Hydrol. Earth Syst. Sci., 22, 5847–5865, https://doi.org/10.5194/hess-22-5847-2018, 2018b.

Gallart, F., Valiente, M., Llorens, P., Cayuela, C., Sprenger, M., and Latron, J.: Investigating young water fractions in a small Mediterranean mountain catchment: Both precipitation forcing and sampling frequency matter, Hydrol. Process., 34, 3618–3634, https://doi.org/10.1002/hyp.13806, 2020a.

Gallart, F., von Freyberg, J., Valiente, M., Kirchner, J. W., Llorens, P., and Latron, J.: Technical note: An improved discharge sensitivity metric for young water fractions, Hydrol. Earth Syst. Sci., 24, 1101–1107, https://doi.org/10.5194/hess-24-1101-2020, 2020b.

© Author(s) 2023. CC BY 4.0 License.

Genereux, D.: Quantifying uncertainty in tracer-based hydrograph separations, Water Resour. Res., 34, 915–919, https://doi.org/10.1029/98WR00010, 1998.

Gentile, A., Canone, D., Ceperley, N., Gisolo, D., Previati, M., Zuecco, G., Schaefli, B., and Ferraris, S.: Towards a conceptualization of the hydrological processes behind changes of young water fraction with elevation: a focus on mountainous alpine catchments, Hydrol. Earth Syst. Sci., 27, 2301–2323, https://doi.org/10.5194/hess-27-2301-2023, 2023.

Harrison, H. N., Hammond, J. C., Kampf, S., and Kiewiet, L.: On the hydrological difference between catchments above and below the intermittent-persistent snow transition, Hydrol. Process., 35, e14411, https://doi.org/10.1002/hyp.14411, 2021.

Hayashi, M., Vogt, T., Mächler, L., and Schirmer, M.: Diurnal fluctuations of electrical conductivity in a pre-alpine river: Effects of photosynthesis and groundwater exchange, J. Hydrol., 450–451, 93–104, https://doi.org/10.1016/j.jhydrol.2012.05.020, 2012.

Hooper, R. P.: Diagnostic tools for mixing models of stream water chemistry, Water Resour. Res., 39, https://doi.org/10.1029/2002WR001528, 2003.

Keller, D. E., Fischer, A. M., Liniger, M. A., Appenzeller, C., and Knutti, R.: Testing a weather generator for downscaling climate change projections over Switzerland, Int. J. Climatol., 37, 928–942, https://doi.org/10.1002/joc.4750, 2017.

Kendall, C. and McDonnell, J. J.: Isotope tracers in catchment hydrology, 1998.

Kiewiet, L., van Meerveld, I., Stähli, M., and Seibert, J.: Do stream water solute concentrations reflect when connectivity occurs in a small, pre-Alpine headwater catchment?, Hydrol. Earth Syst. Sci., 24, 3381–3398, https://doi.org/10.5194/hess-24-3381-2020, 2020.

Kirchner, J. W.: Aggregation in environmental systems-Part 1: Seasonal tracer cycles quantify young water fractions, but not mean transit times, in spatially heterogeneous catchments, Hydrol. Earth Syst. Sci., 20, 279–297, https://doi.org/10.5194/hess-20-279-2016, 2016a.

Kirchner, J. W.: Aggregation in environmental systems-Part 2: Catchment mean transit times and young water fractions under hydrologic nonstationarity, Hydrol. Earth Syst. Sci., 20, 299–328, https://doi.org/10.5194/hess-20-299-2016, 2016b.

Klaus, J. and McDonnell, J. J.: Hydrograph separation using stable isotopes: Review and evaluation, J. Hydrol., 505, 47–64, https://doi.org/10.1016/j.jhydrol.2013.09.006, 2013.

McGuire, K. J. and McDonnell, J. J.: A review and evaluation of catchment transit time modeling, J. Hydrol., 330, 543–563, https://doi.org/10.1016/j.jhydrol.2006.04.020, 2006.

Mosquera, G. M., Segura, C., and Crespo, P.: Flow Partitioning Modelling Using High-Resolution Isotopic and Electrical Conductivity Data, Water, 10, 904, https://doi.org/10.3390/w10070904, 2018.

Nimick, D. A., Gammons, C. H., and Parker, S. R.: Diel biogeochemical processes and their effect on the aqueous chemistry of streams: A review, Chem. Geol., 283, 3–17, https://doi.org/10.1016/j.chemgeo.2010.08.017, 2011.

Penna, D., Engel, M., Bertoldi, G., and Comiti, F.: Towards a tracer-based conceptualization of meltwater dynamics and streamflow response in a glacierized catchment, Hydrol. Earth Syst. Sci., 21, 23–41, https://doi.org/10.5194/hess-21-23-2017, 2017.

Riazi, Z., Western, A. W., and Bende-Michl, U.: Modelling electrical conductivity variation using a travel time distribution approach in the Duck River catchment, Australia, Hydrol. Process., 36, e14721, https://doi.org/10.1002/hyp.14721, 2022.

Schmidt, C., Musolff, A., Trauth, N., Vieweg, M., and Fleckenstein, J. H.: Transient analysis of fluctuations of electrical conductivity as tracer in the stream bed, Hydrol. Earth Syst. Sci., 16, 3689–3697, https://doi.org/10.5194/hess-16-3689-2012, 2012.

Stähli, M., Seibert, J., Kirchner, J. W., von Freyberg, J., and van Meerveld, I.: Hydrological trends and the evolution of catchment research in the Alptal valley, central Switzerland, Hydrol. Process., 35, e14113, https://doi.org/10.1002/hyp.14113, 2021.

https://doi.org/10.5194/egusphere-2023-1797
Preprint. Discussion started: 5 September 2023
© Author(s) 2023. CC BY 4.0 License.

Staudinger, M., Stoelzle, M., Seeger, S., Seibert, J., Weiler, M., and Stahl, K.: Catchment water storage variation with elevation, Hydrol. Process., 31, 2000–2015, https://doi.org/10.1002/hyp.11158, 2017.

Staudinger, M., Seeger, S., Herbstritt, B., Stoelzle, M., Seibert, J., Stahl, K., and Weiler, M.: The CH-IRP data set: a decade of fortnightly data on δ^2H and δ^{18}O in streamflow and precipitation in Switzerland, Earth Syst. Sci. Data, 12, 3057–3066, https://doi.org/10.5194/essd-12-3057-2020, 2020.

Xia, C., Zuecco, G., Chen, K., Liu, L., Zhang, Z., and Luo, J.: The estimation of young water fraction based on isotopic signals: challenges and recommendations, Front. Ecol. Evol., 11, 2023.